Original Article

# Establishing a novel deep learning model for detecting peri-implantitis

Wei-Fang Lee [a,b], Min-Yuh Day [c], Chih-Yuan Fang [a,d],
Vidhya Nataraj [c], Shih-Cheng Wen [a,e], Wei-Jen Chang [a,f],
Nai-Chia Teng [a,g*]

[a] *School of Dentistry, Taipei Medical University, Taipei, Taiwan*
[b] *School of Dental Technology, Taipei Medical University, Taipei, Taiwan*
[c] *Institute of Information Management, National Taipei University, New Taipei City, Taiwan*
[d] *Department of Oral and Maxillofacial Surgery, Wan Fang Hospital, Taipei Medical University, Taipei, Taiwan*
[e] *Private Practice, New Taipei City, Taiwan*
[f] *Dental Department, Taipei Medical University, Shuang Ho Hospital, New Taipei City, Taiwan*
[g] *Department of Dentistry, Taipei Medical University Hospital, Taipei, Taiwan*

**Abstract** Background/purpose: The diagnosis of peri-implantitis using periapical radiographs is crucial. Recently, artificial intelligence may apply in radiographic image analysis effectively. The aim of this study was to differentiate the degree of marginal bone loss of an implant, and also to classify the severity of peri-implantitis using a deep learning model. Materials and methods: A dataset of 800 periapical radiographic images were divided into training ($n = 600$), validation ($n = 100$), and test ($n = 100$) datasets with implants used for deep learning. An object detection algorithm (YOLOv7) was used to identify peri-implantitis. The classification performance of this model was evaluated using metrics, including the specificity, precision, recall, and F1 score. Results: Considering the classification performance, the specificity was 100%, precision was 100%, recall was 94.44%, and F1 score was 97.10%. Conclusion: Results of this study suggested that implants can be identified from periapical radiographic images using deep learning-based object detection. This identification system could help dentists and patients suffering from implant problems. However, more images of other implant systems are needed to increase the learning performance to apply this system in clinical practice.
© 2024 Association for Dental Sciences of the Republic of China. Publishing services by Elsevier B.V. This is an open access article under the CC BY-NC-ND license (http://creativecommons.org/licenses/by-nc-nd/4.0/).

\* Corresponding author. School of Dentistry, Taipei Medical University, No.250, Wuxing St., Xinyi Dist., Taipei City 110, Taiwan.
*E-mail address:* dianaten@tmu.edu.tw (N.-C. Teng).

## Introduction

Since Prof. Branemark completed the first successful mandibular rehabilitation treatment using titanium dental implants in 1965, dental implants have opened a new era in prosthetic treatment for patients with missing teeth or loss of masticatory function.[1,2] Due to its innovative technology, materials, and design, dental implant treatment has become increasingly popular and has significantly grown. According to a survey conducted in the US, the average annual growth rate from 1999 to 2016 was 14%, and it is expected to reach 23% by 2026.[3] As a result, dental implants are the preferred treatment for patients with missing teeth, significantly improving their quality of life.

Numerous studies confirmed that dental implants are an option for restoration, with survival and success rates exceeding 90%.[4,5] However, many complications still occur even 5 years after implant placement, which may lead to implant failure. Implant complications are classified into two categories: mechanical and biological. Mechanical complications include fixture or screw fractures and loosening, as well as implant fractures. Implant mucositis and peri-implantitis are some of the biological complications which occur around the implant.[1,6,7] Researchers have conducted retrospective studies to analyze the numerous risk factors for implant failure, which are attributed to patient factors (such as marginal bone loss and excessive occlusal forces), implant design factors, and restorative factors (such as loosening or fracture of the restoration screw).[8] Further research showed that the incidence of peri-implantitis is as high as 10%~40%,[9–11] and there is a tissue response to plaque formation similar to periodontal disease.[12] Initial symptoms are not obvious and can be overlooked or misdiagnosed. As time passes, it can lead to persistent bone resorption and separation of the implant-bone interface, ultimately resulting in implant loosening or loss and even systemic diseases. Therefore, early diagnosis, accurate staging, and timely and appropriate treatment are crucial for controlling peri-implantitis.

Peri-implant mucositis and peri-implantitis are destructive inflammatory processes that arise pathological conditions in the tissues surrounding dental implants.[13–15] The clinical assessment of peri-implantitis includes the use of a periodontal probe to measure periodontal pocket depth and bleeding, as well as X-ray imaging to detect marginal bone loss (MBL).[14] Alveolar bone loss is typically obscured by periodontal tissues, and it is difficult to directly determine, making x-ray imaging an essential tool for evaluating the range of peri-implant bone loss in cases of peri-implantitis.

Dental x-rays, including two-dimensional (2D) images like periapical (PA) and bitewing, panoramic (Pano), and 3D images like computed tomography (CT) and cone-beam CT (CBCT), are essential tools for diagnosing dental hard-tissue diseases such as caries, periodontal disease, and apical periodontitis. Therefore, x-ray imaging is an important, commonly used tool in dental clinical diagnosis, that plays a crucial role in diagnosing oral hard tissue diseases.[16,17]

Nowadays, artificial intelligence (AI) is flourishing, and applications of radiological image databases in AI systems have made the final diagnosis of various diseases more efficient and accurate. This has become a popular topic in the field of radiology imaging today.[18] In 2010, there was a major breakthrough in intelligent technology with deep learning (DL), where learning models shifted from using graphic processing units (GPUs) to perform classification tasks to using large datasets to execute algorithms for clinical diagnoses, disease predictions, and providing treatment recommendations.[19,20] Convolutional neural networks (CNNs) have been trained to use convolution to extract image features, which enables fast and effective classification and predictions. As a result, CNNs have become popular algorithms for object recognition.[21] In healthcare fields, CNNs are being successfully applied to various types of medical images to resolve different problems. For example, they can automatically assess the shape and position of malignant breast tumors in mammographic images[22,23] and detect diabetic retinopathy in ophthalmological exams.[24]

Diagnosis and treatment in dentistry heavily rely on x-rays, and in recent years, various algorithms have been applied in dentistry, utilizing x-ray images for diagnoses, treatment predictions, classification, and more.[25–28] AI applications have indeed produced satisfactory results in the field of oral medicine. However, up to now, only a few studies are available using DL to detect peri-implantitis in dental x-ray images,[29,30] and no research has explored the relationship between the extent of peri-implantitis and MBL. This method can be used to detect dental implants and peri-implantitis.

Hence, utilizing PA imaging to identify and classify peri-implantitis was the objective of this study. The major purpose was to differentiate the degree of MBL of implants and also classify the severity of peri-implantitis. This was accomplished through automated detection, feature extraction, and categorization, enabling the training of small-scale medical image datasets using DL, resulting in good classification and prediction outcomes.

## Materials and methods

### Image datasets

About 800 anonymized digital PA radiograph images of patients who had experienced dental implant treatment were collected from November 2016 to June 2021 as conducted by the Dental Department of Shuang-Ho Hospital (New Taipei City, Taiwan). In order to prevent personal identification, images were anonymized, and thus, the need for patient consent was waived by the Institutional Review Board of Taipei Medical University (N202103063) for the retrospective collection of images. The study included healthy individuals, excluding those with known systemic diseases.

### Annotation of implants

Three implant systems were physically annotated in periapical radio diagnostic images with an annotation tool (labellmg, Vancouver, British Columbia, Canada). The most commonly used three systems at Shuang-Ho Hospital were selected as dental implants in the present study. These

three implant systems, including Brånemark Mk III System (Nobel Biocare, Zürich, Switzerland, $n = 217$), Implantium Implants System (Dentium CO., LTD, Seoul, South Korea, $n = 360$), and XiVE System (Dentsply Sirona Charlotte, NC, USA, $n = 202$). These were all bone level implants, differing in their connection designs and implant body features.

## Bone loss ratio and classification

Peri-implantitis is determined by the degree of bone loss and other clinical indicators, such as radiographic bone loss and bleeding/suppuration on probing or probing depth.[13,14,31−33] The present study classified the severity of bone loss around implants based on the defect depth at the implant neck and the ratio of bone loss to implant length.[31] Peri-implantitis defects are classified into four groups: Grade 1 < 15% of implant length, Grade 2 ≥ 15%~25% of implant length, Grade 3 ≥ 25%~50% of implant length, and Grade 4 > 50% of implant length (Fig. 1A).

## Data preprocessing and labeling

The images we used were all resized to 640 (width) × 640 (height) pixels, and all of the files were.jpg files, which were used for both training and testing. The images were randomly separated into two datasets: 75% for training (600 images) and 25% for testing and validation (200 images) (Table 1). After learning, models were made by implementing the training dataset. Also, we utilized no image enhancement or pre-processing approaches to improve the PA images, and the test datasets were independent of the training dataset. We assessed the performance of the models which were made using the training dataset.

The labeling process was determined by a dentist with many years of clinical experience, and the labeling decision was made for each image, and then corresponding annotations were generated by the YOLO labeling tool (LabelImg; https://github.com/tzutalin/labelimg). Each implant had three annotated bounding boxes, including the total implant length (the category name of the implant system), a box for bone loss (abbreviated as BL), and a box for non-bone loss (abbreviated as NBL) (Fig. 1B). Annotate bounding boxes on periapical films, marking a rectangle extending from the implant abutment connection to the deepest point of the defect, which appears as a darker area (indicating lower bone density). Then, measure the vertical distance from a predetermined point on the implant. The implant length percentage of the bond defect site over the total implant length, the implant length which not surrounded by bone tissue, and the implant length surrounded by bone tissue were all calculated using coordinates of the three bounding boxes. Then, annotated images were exported in formats of image files (.jpg) and text files (.txt).

## YOLOv7 deep learning network construction and training

The present study used the YOLOv7 DL model whose end-to-end algorithm was proven to achieve high accuracy and rapid analysis of object detection.[34] In this study, YOLOv7 was trained with PA images and their region of interest (ROI) information, and training data were provided with bounding box information for the training phase. The bounding box evidence comprised width (w) and height (h) values, and the class label of the implant in the PA image. The implant system of PA images was detected using a 256 convolutional layer architecture with a variety of kernel sizes, activation functions, skip connections, residual blocks, and fully connected layers.

To implement YOLOv7 for training and testing, pytorch library 2.2.4 was utilized to implement the network and TensorFlow 1.14 (available at https://github.com/tensorflow/tensorflow) which was employed as a desktop backend with a TITAN RTX graphics processing unit (NVIDIA, Santa Clara, CA, USA). YOLOv7 predicted bounding boxes for each grid cell. The YOLO detection procedure splits the input image into 32 × 32 grid cells, each of which detects possible objects in the input image where the center of the object is located. Therefore, each grid cell generates multiple bounding boxes (B) around possible object regions and box confidence scores for whether these boxes contain objects. The training dataset was divided into 32 batches for every epoch, and 1000 epochs were run.

The first part used the Darknet-53 backbone as input with a comma-separated value (CSV), which can provide feature extraction and stacked information from input images. The second part was the spatial pyramid pooling module + path aggregation network (SPP + PAN) which was used to fuse feature evidence of different scales. The third part used YOLO Head for final inspection, which generated final output vectors with object scores, class probabilities, and bounding boxes (Fig. 2).

## Performance metrics

Box confidence was attained by multiplying the probability that a region in the relevant grid cell was an object by the value of the Intersection over union (IOU), as follows:

$$\text{Ground truth confidence} = \text{Prob(object)} \times \text{IOU} \frac{\text{ground truth}}{\text{predicted}}.$$

In this study, total numbers of implants, BLs, and NBLs in all PAs were determined. Objective evaluation of their performances was conducted using the Intersection over union (IOU), a commonly used evaluation metric in object recognition research. The overlap area of the ground-truth bounding box and the predicted bounding box divided by their union area (either ground-truth bounding box or predicted bounding box) was done to calculate the IOU. An IOU threshold value of 0.533 is often set in object detection research, and if the IOU value of a bounding box is greater than 50%, it is considered a true positive (TP); otherwise it is considered a false positive (FP).[35] Multiple bounding boxes were created around possible object regions in each grid cell, and the box confidence score indicated the likelihood that the bounding box contained an object. A confidence score of 0 indicated that there was no object in the corresponding grid cell, and any bounding boxes with zero confidence were therefore excluded. In the present study, "misdetection" refers to the detection of non-MBL loss
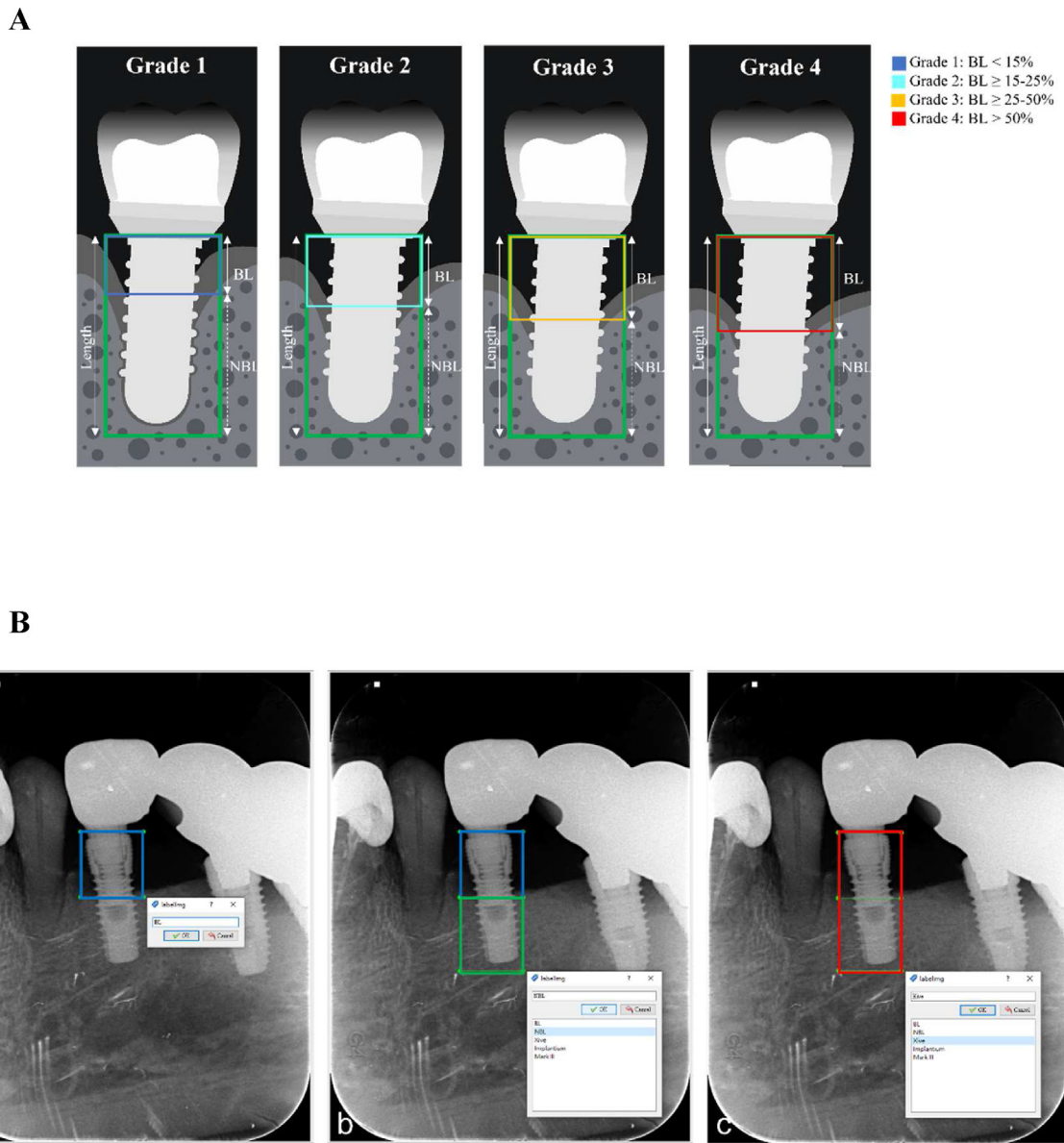
**A**



**B**



**Fig. 1** The classification of peri-implantitis defect grades and the examples by using LabelImg software.
**(A)** Illustration of the classification of peri-implantitis defect grades. Classified to defect severity according to the ratio of marginal bone loss from the total implant length. BL: bone loss; NBL: non-bone loss; Grade 1-4 (%): BL / Total implant length in percentage.
**(B)** Examples of annotating implant fixtures, bone loss, non-bone loss and implant fixture using LabelImg software. a. Marginal bone loss is annotated with blue box. b. Non-bone loss is annotated with green box. c. Xive fixture is annotated with red box.

**Table 1** The number of fixtures for each implant system in the dataset.

| Implant dataset | Xive | Implantium | Mark III | Total |
|---|---|---|---|---|
| Train | 136 | 291 | 173 | 600 |
| Test | 31 | 40 | 29 | 100 |
| Validation | 33 | 37 | 30 | 100 |
| Total dataset | 200 | 368 | 232 | 800 |

areas, while "undetection" refers to failure to accurately detect MBL. This was done to achieve precise MBL detection.

The diagnostic performance of YOLOv7 was measured by the mean average precision (mAP), where a higher value indicates more-accurate learning.[35] Precision, recall, and the F1 score were also used as indicators for evaluating the object detection performance and classification ability. Precision, also called the positive predictive value (PPV), specifies the ability to distinguish negative datasets, with higher precision values indicating stronger discriminative ability. Recall, also called sensitivity or the true positive rate (TPR), specifies the ability of a model to interpret positive datasets, with higher recall values indicating a better performance with positive datasets. A higher recall
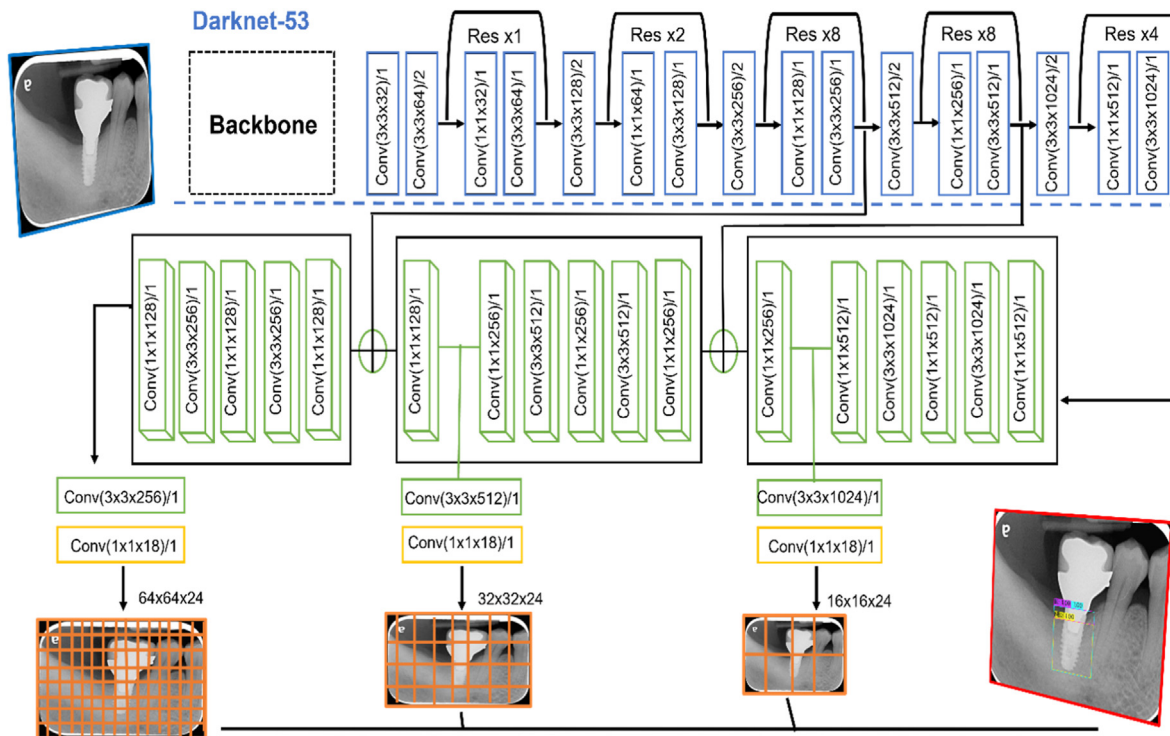
**Fig. 2**    Structure of YOLOv7 used in the study.

score may lead to a lower precision score, and it is unclear whether a higher precision score or recall score is better.

Considering the overall evaluation of the classification performance, based on the yielded TP, true negative (TN), FP, and false negative (FN) values, the accuracy, precision, recall, specificity, and F1 score were respectively calculated and are shown in Table 2. Table 2 also summarizes the predicted and actual results used to determine the accuracy of the model. The accuracy, sensitivity, specificity, precision, and F1 score were calculated as follows:

$$Accuracy = [TP + TN] / [TP + TN + FP + FN];$$

$$Sensitivity = TP / (TP + FN);$$

$$Specificity = TN / (TN + FP);$$

$$Precision = TP / (TP + FP);$$

$$F1\text{-}score = 2 \times precision \times recall / (precision + recall).$$

**Table 2**    Accuracy, sensitivity, specificity, precision, and F1 score values for recognizing peri-implantitis.

|  | Accuracy | Precision | Sensitivity | Specificity | F1-Score |
|---|---|---|---|---|---|
| Overall | 94.74% | 100% | 94.44% | 100% | 97.10% |
| Bone loss | 96.18% | 100% | 95.83% | 100% | 97.86% |
| Non-bone loss | 93.42% | 100% | 93.06% | 100% | 96.43% |

## Results

### Dental implant system classification

Various results of the implant detection system of at least 200 images were recognized in periapical radiographic images, and the implant type with the maximum number was Implantium (368), while the minimum implant type was Xive (200). Table 1 provides information on the implants in the training, test, and validation datasets. Fig. 3 provides information of the peri-implantitis defect grades in the datasets.

### YOLOv7 model performance results for BL classifications

From observations, a few of the diagnoses were missed, but the area of BL as determined by YOLOv7 was usually similar to the ground truth bounding box. The YOLOv7 model and the observer annotations converged with an increase in the severity of BL.

TP, TN, FP and FN values, and the accuracy, sensitivity, specificity, and F1 score were calculated and are shown in Table 2. Table 2 also summarizes the predicted and actual results used to determine the accuracy of the model. Ratios in Implantium and Xive implants were the largest accuracy at 0.98, while that in Mark III implants was the smallest at 0.97. Performance metrics of the YOLOv7 model for recognizing peri-implantitis in a total of 800 periapical images were an accuracy of 94.74%, a sensitivity of 94.44%, and an F1 score of 97.10%. There was no statistically significant difference in the classification accuracy observed
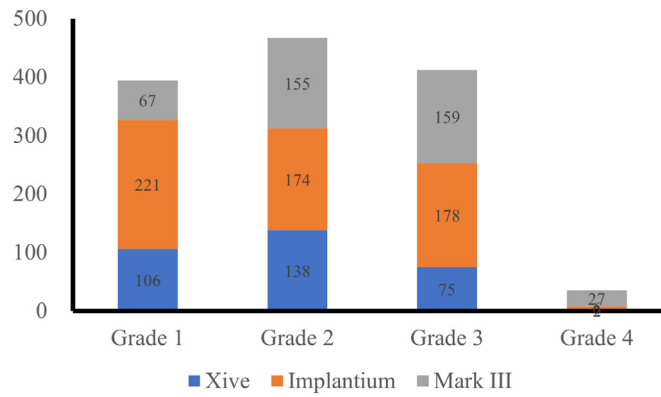
**Fig. 3** The number of peri-implantitis defect grades in the dataset.

among the three groups, and the detailed accuracy performances of YOLOv7 are given in Table 2.

## Confusion matrix

Other results analyzed were a confusion matrix of BL and NBL based on the YOLOv7 architecture for model training and testing as shown in Fig. 4. According to the quantity of correct values with the arrangement, the color gamut of shades varied and became darker. The diagonal components are the quantity of images appropriately predicted, and the label of the prediction matches the true label.

## Discussion

Removing a failed dental implant and replacing it with a new one is expensive and technically challenging. Regenerative treatments for dental implant repair can also be costly and unpredictable if not done correctly. Long-term maintenance and clinical oversight of peri-implant disease remain the most cost-effective and successful preventive measures for treating this disease.[36] After implant placement and abutment connection, limited BL may occur. This

biological process may lead to unwanted implant surface exposure and biofilm adherence. Early BL is a risk factor for peri-implantitis, according to a large study population. The higher the amount of early BL, the higher the incidence of disease, especially in combination with other risk factors such as smoking.[37]

According to a recent study, peri-implantitis is classified into three groups based on the severity of BL. The groups are as follows: stage 1: BL $<$ 25% (of fixture length), stage 2: 25% $<$ BL $<$ 50%, and stage 3: BL $>$ 50%.[38] A dentist needs to locate appropriate landmarks to analyze radio diagnostic images and diagnose peri-implantitis. However, as discussed in previous studies, the severity of peri-implantitis is classified depending on the degree of BL based on the percentage of radiographic BL.[39,40] According to the 2017 World Workshop on the classification of peri-implant and periodontal diseases and conditions,[13] the evidence suggested that if there is an increased risk of developing peri-implantitis at sites, probing depth was correlated with BL and was, hence, an indicator for the severity of disease. Problems like implant detection and peri-implantitis remain unsolved in general clinics in the field of dentistry. In this case, an unknown implant system, degree of marginal bone, and the severity of peri-implantitis will make
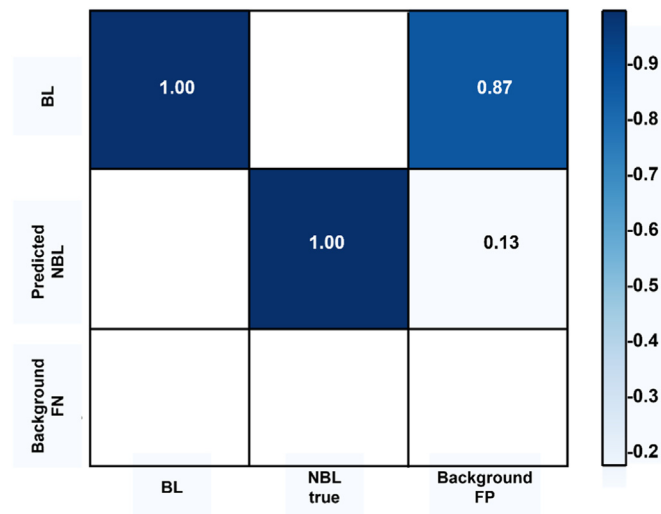


**Fig. 4** Confusion matrix of YOLOv7.

problems worse and result in other serious dental problems. Therefore, identifying MBL and the dental implant system is essential for both dentists and patients.

Digital radiographs are most effective for identifying MBL and peri-implantitis. This is the starting point for the evaluation and finding more-convenient ways in daily clinical settings. To identify implant systems, radiographs of implants are suggested after physiological remodeling to assess changes in the bone level.[39,41] A certain level can be standardized regardless of the patient, and standardized shapes of implants in images are an advantage of using PA radiographic images. Studies suggest that PA radiographs are the most reliable way to capture the entire tooth to the root apex with minimal distortion, and they can detect peri-implant BL.[42] This study was conducted using digital PA images, and datasets were divided into training, validation, and test datasets. This study focused on automated identification and classification of MBL of dental systems and the severity of the peri-implantitis from PA radiographic images utilizing a DL-based model, an AI technique. Thus, the model itself identified the implant rather than the dentist. Trained algorithms were tested for their performance using the test dataset.

Takahashi et al. applied an object detection model called YOLOv3 to identify six different dental implant systems using a total of 1282 pano-radiograph images.[43] While the detection of a large number of implants is noteworthy, it is important to highlight that only implant regions devoid of peri-implant tissue were successfully detected, and an mAP of 0.71 they used is a relatively inadequate level of accuracy. This outcome was due to the fact that they utilized pano-radiographs, which have lower image quality compared to periapical radiographs utilized in this study.

AI technologies are being clinically assessed in the terms of the diagnostic performance and patient results, and also many professionals have confidence that AI techniques will progressively replace or be substituted for medical education for healthcare experts, particularly in diagnoses.[40,44] Differentiating the degree of MBL of implants and classifying the severity of peri-implantitis are of often challenging. In view of the serious issues involved, an automated AI-based method will be a good resolution to prevent further complications and causes. Furthermore, the CNN took 38 s and oral maxillofacial specialists took 23.1 min for a diagnosis, demonstrating AI's efficiency.[45] In our study, we used a CNN which exhibited good accuracy, and we concluded that the CNN model can facilitate detection of MBL around implants. A study reported that YOLOv7 had the highest accuracy in real time object detection in terms of both accuracy and speed.[34]

The YOLOv7 model was used in this study for detection and classification, while Chat et al., used the Mask Regional-CNN (R—CNN) model that detects and classifies target frames and then segments targets at pixel levels.[29] The implants were recognized and categorized according to the brand name with high accuracy by the AI system. Also, an automated identification system which is not dependent on the dentist's expertise is required. In this study, we divided MBL training data according to the implant abutment connection type, and BL areas were automatically identified by the model (Fig. 1B).

Several metrics of diagnostic performance were used for model evaluation. When estimating the performance of object detection, mAP and IOU are mainly used, also precision, recall, and F1 score are used. The accuracy of the object detection model was measured employing mAP. A mAP value of closer to 1.0 is considered more accurate.[35] An IOU value of a bounding box of greater than 50% is considered a TP, and the mAP obtained in this study was 0.94. Thus, on account of this, the performance of the hyperparameters was determined to be high.

In implant detection among all ground truth labels, we included all of the dental implants within the entire test dataset. Considering the FP and FN, the FN was not able to detect the implant profile that was truncated in the corner of the image. If a PA radiograph clearly provides all of the profiles of an implant, a higher accuracy would be predicted. Meanwhile, when brightness and saturation within
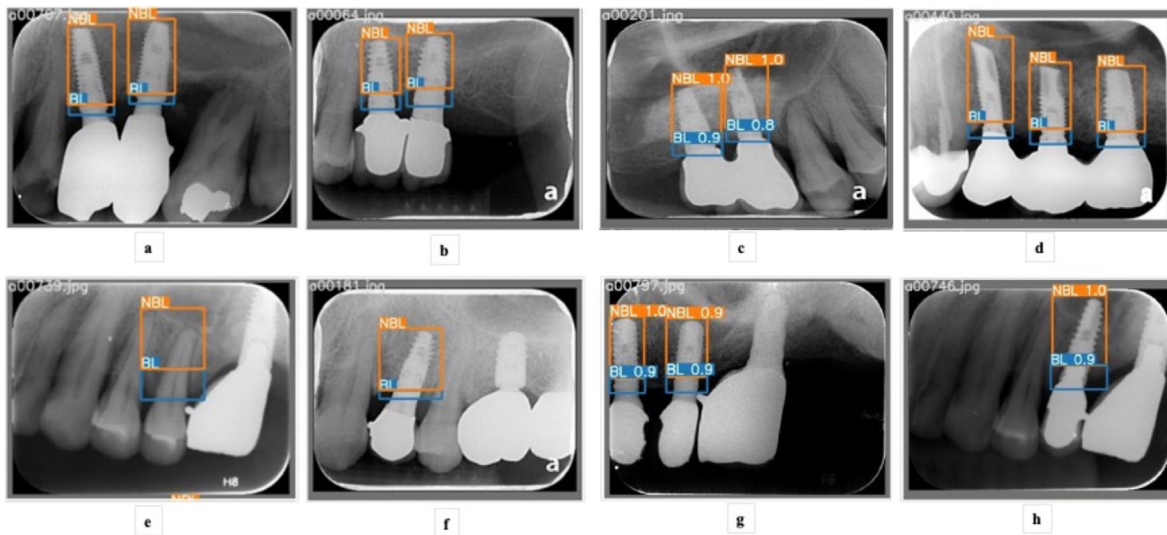


**Fig. 5** Example images of the result of the marginal bone loss detection test. a—d: True positive (TP) cases that well detected dental implants and peri-implantitis, e: false positive (FP) cases, f—h: false negative (FN) cases.

the images were similar to those of implants such as crowns and pontics, an FN can occur (Fig. 5).

Prevention is key when it comes to peri-implantitis. Clinicians should carefully monitor patients who are at risk for biological complications and identify risk factors/indicators to categorize an individual patient for his/her susceptibility. This may also alter the maintenance protocol in order to prevent complications. For patients exhibiting early BL exceeding a certain threshold, stricter monitoring may be advantageous to prevent further development of biological complications.[46,47]

According to a systematic review and meta-analysis, all implants produce some degree of BL following implant installation and loading. Early implant BL of 1.5 mm occurs during the healing phase and the first year in function at the crestal area of implants, followed by annual BL of 0.2 mm thereafter. One study also found that implant neck design and surface characterization were associated with reduced MBL.[48] Detection of the brand of the implant system is important as well as the BL level. Clinicians should closely monitor the patient for peri-implant BL or a change in the implants' response to percussion after implant placement. A retrospective study found that radiological evaluation of MBL can be performed in different ways, such as by evaluating the distance from the implant shoulder to the bone or by measuring the number of exposed threads that are not in contact with bone.[49] The brand of the implant might influence the amount of early bone loss around the implant, which may necessitate further investigation into the variations in surface treatment and implant design. Further study for detecting both the implant system and BL will be important for AI detection systems.

In our study, we used a CNN and achieved good accuracy. We concluded that the CNN model can facilitate detection of MBL around implants. According to studies, YOLOv7 had the highest accuracy and speed in real-time object detection. Further study for detecting both the implant system and BL will be important for AI detection systems. This can help clinicians monitor a patient's condition more accurately and efficiently.

## Declaration of competing interest

The authors have no conflicts of interest relevant to this article.

## Acknowledgments

## References

1. Howe MS, Keys W, Richards D. Long-term (10-year) dental implant survival: a systematic review and sensitivity meta-analysis. *J Dent* 2019;84:9—21.
2. Branemark PI, Zarb GA, Albrektsson T. Tissue-integrated prostheses. *Quintessence* 1985;1:99—115.
3. Elani H, Starr J, Da Silva J, Gallucci G. Trends in dental implant use in the US, 1999—2016, and projections to 2026. *J Dent Res* 2018;97:1424—30.
4. Srinivasan M, Vazquez L, Rieder P, Moraguez O, Bernard JP, Belser UC. Survival rates of short (6 mm) micro-rough surface implants: a review of literature and meta-analysis. *Clin Oral Implants Res* 2014;25:539—45.
5. Ramanauskaite A, Borges T, Almeida BL, Correia A. Dental implant outcomes in grafted sockets: a systematic review and meta-analysis. *J Oral Maxillofac Res* 2019;10:1—13.
6. Moraschini V, Poubel LdC, Ferreira V, dos Sp Barboza E. Evaluation of survival and success rates of dental implants reported in longitudinal studies with a follow-up period of at least 10 years: a systematic review. *Int J Oral Maxillofac Surg* 2015;44: 377—88.
7. Srinivasan M, Meyer S, Mombelli A, Müller F. Dental implants in the elderly population: a systematic review and meta-analysis. *Clin Oral Implants Res* 2017;28:920—30.
8. Stoichkov B, Kirov D. Analysis of the causes of dental implant fracture: a retrospective clinical study. *Quintessence Int* 2018; 49:279—86.
9. Derks J, Schaller D, Håkansson J, Wennström J, Tomasi C, Berglundh T. Effectiveness of implant therapy analyzed in a Swedish population: prevalence of peri-implantitis. *J Dent Res* 2016;95:43—9.
10. Rodrigo D, Sanz-Sánchez I, Figuero E, et al. Prevalence and risk indicators of peri-implant diseases in Spain. *J Clin Periodontol* 2018;45:1510—20.
11. Romandini M, Lima C, Pedrinaci I, Araoz A, Soldini MC, Sanz M. Prevalence and risk/protective indicators of peri-implant diseases: a university-representative cross-sectional study. *Clin Oral Implants Res* 2021;32:112—22.
12. Zitzmann N, Berglundh T, Marinello C, Lindhe J. Experimental peri-implant mucositis in man. *J Clin Periodontol* 2001;28: 517—23.
13. Schwarz F, Derks J, Monje A, Wang HL. Peri-implantitis. *J Clin Periodontol* 2018;45:S246—66.
14. Atieh MA, Alsabeeha NH, Faggion Jr CM, Duncan WJ. The frequency of peri-implant diseases: a systematic review and meta-analysis. *J Periodontol* 2013;84:1586—98.
15. Berglundh T, Armitage G, Araujo MG, et al. Peri-implant diseases and conditions: consensus report of workgroup 4 of the 2017 world Workshop on the classification of periodontal and peri-implant diseases and conditions. *J Periodontol* 2018;89: S313—8.
16. Affairs. The use of dental radiographs: update and recommendations. *J Am Dent Assoc* 2006;137:1304—12.
17. Kühl S, Zürcher S, Zitzmann NU, Filippi A, Payer M, Dagassan-Berndt D. Detection of peri-implant bone defects with different radiographic techniques—a human cadaver study. *Clin Oral Implants Res* 2016;27:529—34.
18. Recht M, Bryan RN. Artificial intelligence: threat or boon to radiologists? *J Am Coll Radiol* 2017;14:1476—80.
19. Chan YK, Chen YF, Pham T, Chang W, Hsieh MY. Artificial intelligence in medical applications. *J Healthc Eng* 2018;2018: 4827875.
20. Aizenberg IN, Aizenberg NN, Vandewalle JP. *Multi-valued and universal binary neurons: theory, learning and applications*. Springer Science & Business Media, 2013.
21. Litjens G, Kooi T, Bejnordi BE, et al. A survey on deep learning in medical image analysis. *Med Image Anal* 2017;42:60—88.
22. Al-Masni MA, Al-Antari MA, Park JM, et al. Simultaneous detection and classification of breast masses in digital mammograms via a deep learning YOLO-based CAD system. *Comput Methods Progr Biomed* 2018;157:85—94.
23. Becker AS, Marcon M, Ghafoor S, Wurnig MC, Frauenfelder T, Boss A. Deep learning in mammography: diagnostic accuracy of

a multipurpose image analysis software in the detection of breast cancer. *Invest Radiol* 2017;52:434—40.

24. Gulshan V, Peng L, Coram M, et al. Development and validation of a deep learning algorithm for detection of diabetic retinopathy in retinal fundus photographs. *JAMA* 2016;316:2402—10.

25. Lee JH, Kim DH, Jeong SN, Choi SH. Detection and diagnosis of dental caries using a deep learning-based convolutional neural network algorithm. *J Dent* 2018;77:106—11.

26. Krois J, Ekert T, Meinhold L, et al. Deep learning for the radiographic detection of periodontal bone loss. *Sci Rep* 2019; 9:1—6.

27. Schwendicke F, Golla T, Dreher M, Krois J. Convolutional neural networks for dental image diagnostics: a scoping review. *J Dent* 2019;91:103226.

28. Son DM, Yoon YA, Kwon HJ, An CH, Lee SH. Automatic detection of mandibular fractures in panoramic radiographs using deep learning. *Diagnostics* 2021;11:933.

29. Cha JY, Yoon HI, Yeo IS, Huh KH, Han JS. Peri-implant bone loss measurement using a region-based convolutional neural network on dental periapical radiographs. *J Clin Med* 2021;10:1009.

30. Mameno T, Wada M, Nozaki K, et al. Predictive modeling for peri-implantitis by using machine learning techniques. *Sci Rep* 2021;11:11090.

31. Monje A, Pons R, Insua A, Nart J, Wang HL, Schwarz F. Morphology and severity of peri-implantitis bone defects. *Clin Implant Dent Relat Res* 2019;21:635—43.

32. Ravidà A, Galli M, Siqueira R, Saleh MH, Galindo-Moreno P, Wang HL. Diagnosis of peri-implant status after peri-implantitis surgical treatment: proposal of a new classification. *J Periodontol* 2020;91:1553—61.

33. Tonetti MS, Greenwell H, Kornman KS. Staging and grading of periodontitis: framework and proposal of a new classification and case definition. *J Periodontol* 2018;89:S159—72.

34. Wang CY, Bochkovskiy A, Liao HYM. YOLOv7: trainable bag-of-freebies sets new state-of-the-art for real-time object detectors. *arXiv preprint arXiv* 2022:220702696.

35. Zhao ZQ, Zheng P, Xu ST, Wu X. Object detection with deep learning: a review. *IEEE Transact Neural Networks Learn Syst* 2019;30:3212—32.

36. Bernard S, Kotsailidi EA, Chochlidakis K, Ercoli C, Tsigarida A. Implant and peri-implant tissue maintenance: protocols to prevent peri-implantitis. *Curr Oral Health Rep* 2020;7:249—61.

37. Windael S, Collaert B, De Buyser S, De Bruyn H, Vervaeke S. Early peri-implant bone loss as a predictor for peri-implantitis: a 10-year prospective cohort study. *Clin Implant Dent Relat Res* 2021;23:298—308.

38. Hwang S, Lee HM, Yun PY, Kim YK. Survival analysis of implants after surgical treatment of peri-implantitis based on bone loss severity and surgical technique: a retrospective study. *BMC Oral Health* 2023;23:308.

39. Sanz M, Chapple IL, Working Group 4 of the VEWoP. Clinical research on peri-implant diseases: consensus report of Working Group 4. *J Clin Periodontol* 2012;39:202—6.

40. Liu X, Faes L, Kale AU, et al. A comparison of deep learning performance against health-care professionals in detecting diseases from medical imaging: a systematic review and meta-analysis. *Lancet Digit Health* 2019;1:e271—97.

41. Nuzzolese E, Lusito S, Solarino B, Di Vella G. Radiographic dental implants recognition for geographic evaluation in human identification. *J Forensic Odontostomatol* 2008;26: 11—8.

42. Liu M, Wang S, Chen H, Liu Y. A pilot study of a deep learning approach to detect marginal bone loss around implants. *BMC Oral Health* 2022;22:11.

43. Takahashi T, Nozaki K, Gonda T, Mameno T, Wada M, Ikebe K. Identification of dental implants using deep learning—pilot study. *Int. J. Implant Dent.* 2020;6:1—6.

44. Park SH, Kressel HY. Connecting technological innovation in artificial intelligence to real-world medical practice through rigorous clinical validation: what peer-reviewed medical journals could do. *J Kor Med Sci* 2018;33:e152.

45. Poedjiastoeti W, Suebnukarn S. Application of convolutional neural network in the diagnosis of jaw tumors. *Healthc Inform Res* 2018;24:236—41.

46. Windael S, Vervaeke S, De Buyser S, De Bruyn H, Collaert B. The long-term effect of smoking on 10 years' survival and success of dental implants: a prospective analysis of 453 implants in a non-university setting. *J Clin Med* 2020;9:1056.

47. Albrektsson T, Buser D, Chen ST, et al. Statements from the Estepona consensus meeting on peri-implantitis. *Clin Implant Dent Relat Res* 2012;14:781—2.

48. Koodaryan R, Hafezeqoran A. Evaluation of implant collar surfaces for marginal bone loss: a systematic review and meta-analysis. *BioMed Res Int* 2016:4987526.

49. Castellanos-Cosano L, Carrasco-García A, Corcuera-Flores JR, Silvestre-Rangil J, Torres-Lagares D, Machuca-Portillo G. An evaluation of peri-implant marginal bone loss according to implant type, surgical technique and prosthetic rehabilitation: a retrospective multicentre and cross-sectional cohort study. *Odontology* 2021;109:649—60.